Reflection and Transmission of Plane Waves at an Interface between Elastic and Micropolar Piezoelectric Solid Half-Spaces

A. Sangwan, B. Singh[*], J. Singh

A problem of reflection and transmission of elastic waves at an interface between an elastic solid half-space and a micropolar piezoelectric solid half-space is considered. Both the half-spaces are assumed to be transversely isotropic. For an incident wave from transversely isotropic elastic solid half-space, two reflected waves in transversely isotropic elastic half-space and three transmitted waves in transversely isotropic micropolar piezoelectric solid half-space exist. The appropriate potentials of incident, reflected and transmitted waves satisfy the required boundary conditions at interface and relations in amplitude ratios of all reflected and transmitted waves are obtained with a suitable Snell's law. The expressions for energy ratios of various reflected and transmitted waves are also obtained. The amplitude ratios and the square root of energy ratios of reflected and transmitted waves are computed numerically for a particular material representing the present model. The amplitude ratios and the square root of energy ratios are plotted against the angle of incidence to observe the effect of micropolar piezoelectricity.

1   Introduction

During recent decades, the subject of vibrations, wave propagation and their reflection and transmission from interfaces in an elastic medium is of great interest. Mathematical treatment of reflection and transmission of a plane wave at the interface between two dissimilar media is a fundamental topic in many fields such as seismology, geophysics, earthquake engineering, non-destructive evaluation etc. Such problems are intensively studied for both isotropic and anisotropic elastic solids. These studies provide useful information about the internal composition of the Earth and, in addition, are important in exploration of valuable materials beneath the Earth surface, e.g., water, oils, minerals, hydro-carbons, etc. The problems of the reflection and refraction of elastic waves in layered media have been discussed by several authors including Knott (1899), Jeffreys (1926), Gutenberg (1944), Ergin (1950), Ewing et al. (1957) and Achenbach (1973).

Micropolar theory is an extension of elasticity with extra independent degrees of freedom for local rotation. In micropolar theory, each particle has a finite size and contains a microstructure, which can rotate. In this theory, the motions of the particles are expressed in terms of displacement and micro-rotation vector. Eringen (1966, 1968) introduced the linear theory of micropolar elasticity and explained the micro-rotational motion and spin inertia that can support coupled stress and body couples in materials. He (1999, 2012) introduced the micro-continuum field theories of solids, including electromagnetic and thermal interactions. Many problems of wave and vibrations of micropolar elasticity have been investigated by several researchers (Smith, 1967; Perfitt and Eringen, 1969; Ariman, 1972; Nowacki, 1986; Tomar and Gogna, 1995; Eremeyev and Lebedev, 2013; Singh and Goyal, 2017).

The materials possessing linear coupling between mechanical and electric fields are termed as piezoelectric materials. These materials find their utility as sensors and actuators in many applications involving signal transmission. In the past two decades, the reflection/refraction problems of piezoelectric materials received considerable attention. The propagation of plane waves in such materials was studied by various authors, for example, Kyame (1949), Pailloux (1958), Hruska (1966) and Auld (1973). Different researchers have studied the problems of reflection and transmission in piezoelectric media notable among them are Chai and Wu (1966), Wang (2002), Yang (2006), Pang et al. (2008), Abd-alla and Al-sheikh (2009 a, b), Singh (2010), Kuang and Yuan (2011), Yuan and Zhu (2012) and Guo and Wei (2014). Micropolar piezoelectricity has not been explored much till date. Few problems in micropolar piezoelectric medium have been investigated. Cracium (1995) formulated the basic equations of the linear theory of piezoelectric micropolar thermoelasticity with quasi-static

electric fields. Ciumasu and Vieru (1999) presented the variational formulation for the free vibration of a micropolar piezoelectric body. Zhilin and Kolpakov (2005) developed the theory of the micropolar piezoelectric materials and formulated the basic equations of micropolar piezoelectricity. Aouadi (2008) considered the linear dynamic theory of micropolar piezoelectricity and established a reciprocity relation with two processes at different instants. Huang and Yu (2010) analysed size effect of a crack in a micropolar piezoelectric medium. Gales (2012) considered the linear theory of micromorphic piezoelectricity and formulated the initial boundary value problem and presented some uniqueness results. Recently, Singh and Sindhu (2016) studied the propagation of Rayleigh waves in micropolar piezoelectric medium.

The present work extends the existing studies of the wave reflection and transmission problem in piezoelectric medium by introducing concept of micropolarity. The problem of reflection and transmission at an interface between elastic and micropolar piezoelectric half-spaces is not attempted so far. In the present paper, the reflection and transmission phenomenon at a plane interface between a transversely isotropic elastic medium and a transversely isotropic micropolar piezoelectric medium in welded contact is considered. The governing equations of both the media are specialized in x-z plane and their plane wave solutions indicate the existence of two quasi-plane waves in transversely isotropic elastic medium and three quasi-plane waves in micropolar piezoelectric medium. The appropriate potentials for incident, reflected and transmitted waves in both half-spaces are obtained, which satisfy required boundary conditions at interface. The relations in amplitude ratios and the expressions for energy ratios of reflected and transmitted waves in both media are obtained analytically. A numerical example of the model is considered to compute the square root of the energy ratios of reflected and transmitted waves. The results are compared with those for an interface between two dissimilar transversely isotropic elastic half-spaces to observe the effect of micropolar piezoelectricity on the ratios.

2 Basic Equations

Following Aouadi (2008), the fundamental system of field equations for the linear theory of micropolar piezoelectric solids in the absence of body forces and body couples consists of the equations of the motion

$$\sigma_{ji,j} = \rho \ddot{u}_i , \tag{1}$$

$$m_{ik,i} + \varepsilon_{ijk}\sigma_{ij} = \rho j \ddot{\phi}_k , \tag{2}$$

the equations of the electric fields

$$D_{j,j} = q_e , \quad E_k = -\psi_{,k} , \tag{3}$$

the constitutive equations

$$\sigma_{ij} = c_{ijkl}e_{kl} + b_{ijkl}\kappa_{kl} + \lambda_{ijk}E_k , \tag{4}$$

$$m_{ij} = b_{klij}e_{kl} + a_{ijkl}\kappa_{kl} + \beta_{ijk}E_k , \tag{5}$$

$$D_k = -\lambda_{ijk}e_{ij} - \beta_{ijk}\kappa_{ij} + \gamma_{kj}E_j , \tag{6}$$

and the geometrical equations

$$e_{ij} = u_{j,i} + \varepsilon_{ijk}\phi_k , \quad \kappa_{ij} = \phi_{j,i} . \tag{7}$$

where σ_{ij} is the stress tensor, ρ is the mass density, $\vec{u}$ is the displacement vector, $\vec{\phi}$ is the microrotation vector, j is the micro-inertia, m_{ij} is the couple stress tensor, ε_{ijk} is the alternating symbol, D_k is the dielectric displacement vector, q_e is the volume charge density, E_j is the electric field vector, ψ is the electrostatic potential, e_{ij} and κ_{ij} are kinematic strain measures and $a_{ijkl}, b_{ijkl}, c_{ijkl}, \lambda_{ijk}, \beta_{ijk}$ and γ_{jk} are constitutive coefficients. Superposed dot denote partial differentiation with respect to the time t. Subscripts preceded by a comma denote partial differentiation with respect to the corresponding Cartesian coordinate and the repeated

index in the subscript implies summation. It is also assumed in Aouadi (2008) that the constitutive coefficients satisfy the symmetry relations

$$c_{ijkl} = c_{klij}, \ a_{ijkl} = a_{klij}, \ \gamma_{ij} = \gamma_{ji}. \tag{8}$$

3 Formulation of the Problem and Plane Wave Solutions

We consider a homogeneous transversely isotropic elastic half-space lying over a homogeneous transversely isotropic micropolar piezoelectric half-space in welded contact. The origin of the Cartesian coordinate system (x, y, z) is taken at any point on the plane interface and z-axis points vertically downwards into micropolar piezoelectric half-space. The elastic solid half-space occupies the region $z \leq 0$ (medium M') and the region $z \geq 0$ is occupied by the micropolar piezoelectric half-space (medium M) as shown in Fig. 1. We consider plane waves in the x-z plane with wave front parallel to the y-axis. For two-dimensional problem, the displacement vector $\vec{u}'$ in medium M' and displacement vector $\vec{u}$ and microrotation vector $\vec{\phi}$ in medium M are taken as

$$\vec{u}' = \left(u_1', 0, u_3'\right), \ \vec{u} = \left(u_1, 0, u_3\right) \ \text{and} \ \vec{\phi} = \left(0, \phi_2, 0\right). \tag{9}$$

Using equations (1) to (9), the equations of motion for transversely isotropic micropolar piezoelectric medium M are expressed as

$$A_{11}\frac{\partial^2 u_1}{\partial x^2} + \left(A_{13} + A_{56}\right)\frac{\partial^2 u_3}{\partial x \partial z} + A_{55}\frac{\partial^2 u_1}{\partial z^2} + K_1\frac{\partial \phi_2}{\partial z} - \left(\lambda_{15} + \lambda_{31}\right)\frac{\partial^2 \psi}{\partial x \partial z} = \rho\frac{\partial^2 u_1}{\partial t^2}, \tag{10}$$

$$A_{66}\frac{\partial^2 u_3}{\partial x^2} + \left(A_{13} + A_{56}\right)\frac{\partial^2 u_1}{\partial x \partial z} + A_{33}\frac{\partial^2 u_3}{\partial z^2} + K_2\frac{\partial \phi_2}{\partial x} - \lambda_{15}\frac{\partial^2 \psi}{\partial x^2} - \lambda_{33}\frac{\partial^2 \psi}{\partial z^2} = \rho\frac{\partial^2 u_3}{\partial t^2}, \tag{11}$$

$$B_{77}\frac{\partial^2 \phi_2}{\partial x^2} + B_{66}\frac{\partial^2 \phi_2}{\partial z^2} - \chi\phi_2 - K_1\frac{\partial u_1}{\partial z} - K_2\frac{\partial u_3}{\partial x} - \beta_{14}\frac{\partial^2 \psi}{\partial x^2} - \beta_{36}\frac{\partial^2 \psi}{\partial z^2} = \rho j\frac{\partial^2 \phi_2}{\partial t^2}, \tag{12}$$

$$\lambda_{15}\frac{\partial^2 u_3}{\partial x^2} + \lambda_{33}\frac{\partial^2 u_3}{\partial z^2} + \left(\lambda_{15} + \lambda_{31}\right)\frac{\partial^2 u_1}{\partial x \partial z} + \beta_{14}\frac{\partial^2 \phi_2}{\partial x^2} + \beta_{36}\frac{\partial^2 \phi_2}{\partial z^2} + \gamma_{11}\frac{\partial^2 \psi}{\partial x^2} + \gamma_{33}\frac{\partial^2 \psi}{\partial z^2} = 0, \tag{13}$$

where

$$A_{11} = C_{1111}, A_{55} = C_{3131}, A_{13} = C_{1133} = C_{3311}, A_{56} = C_{3113} = C_{1331}, A_{66} = C_{1313},$$
$$A_{33} = C_{3333}, K_1 = A_{56} - A_{55} = C_{3113} - C_{3131}, K_2 = A_{66} - A_{56} = C_{1313} - C_{1331},$$
$$\chi = K_2 - K_1, B_{77} = a_{1212}, B_{66} = a_{3232}, \lambda_{31} = \lambda_{311}, \lambda_{33} = \lambda_{333},$$
$$\lambda_{15} = \lambda_{131} = \lambda_{113}, \lambda_{35} = \lambda_{313} = \lambda_{331}, \beta_{14} = \beta_{121}, \beta_{36} = \beta_{323}.$$

We seek the plane wave solution of the equations (10) to (13) in the following form

$$\{u_1, u_3, \phi_2, \psi\} = (A, B, C, D) \exp.\{ik(x\sin\theta + z\cos\theta - vt)\}. \tag{14}$$

where k is the wave number and v is the speed of wave propagating in x-z plane along a direction making an angle θ with z-axis.

Making use of equation (14) in equations (10-13), we obtain four homogeneous equations in A, B, C and D and which have non-trivial solution if

$$\Gamma^3 - S_1\Gamma^2 + S_2\Gamma - S_3 = 0 \tag{15}$$

where

$$\Gamma = \rho v^2,$$
$$S_1 = (D_1 D_6 + D_2 D_6 + D_3^2 + L_2^2 + D_4^* D_6 + D_5 D_5^*)/D_6,$$

$$S_2 = [D_1 D_2 D_6 + (D_1 + D_4^*) D_3^2 + (D_2 + D_4^*) L_2^2 - D_6 L_1^2 - 2L_1 L_2 D_3$$
$$+ (D_1 + D_2)(D_4^* D_6 + D_5 D_5^*) - K_2 K_2^* D_6 \sin^2 \theta - K_1 K_1^* D_6 \cos^2 \theta] \cdot D_6^{-1},$$

$$S_3 = [(D_1 D_2 - L_1^2)(D_4^* D_6 + D_5 D_5^*) + D_1 D_3^2 D_4^* + D_2 D_4^* L_2^2 - 2L_1 L_2 D_3 D_4^* - (D_1 D_6 + L_2^2) K_2 K_2^* \sin^2 \theta$$
$$- (D_2 D_6 + D_3^2) K_1 K_1^* \cos^2 \theta + 2(L_1 D_6 + L_2 D_3) K_1 K_2^* \sin \theta \cos \theta] \cdot D_6^{-1},$$

$$D_1 = A_{11} \sin^2 \theta + A_{55} \cos^2 \theta, \ D_2 = A_{66} \sin^2 \theta + A_{33} \cos^2 \theta, \ D_3 = \lambda_{15} \sin^2 \theta + \lambda_{33} \cos^2 \theta,$$

$$D_4 = B_{77} \sin^2 \theta + B_{66} \cos^2 \theta, \ D_4^* = \frac{D_4}{j} + \frac{\chi}{jk^2}, \ D_5 = \beta_{14} \sin^2 \theta + \beta_{36} \cos^2 \theta, \ D_5^* = \frac{D_5}{j},$$

$$D_6 = \gamma_{11} \sin^2 \theta + \gamma_{33} \cos^2 \theta, \ L_1 = (A_{13} + A_{56}) \sin \theta \cos \theta, \ L_2 = (\lambda_{15} + \lambda_{31}) \sin \theta \cos \theta,$$

$$K_1^* = \frac{K_1}{jk^2}, \ K_2^* = \frac{K_2}{jk^2}.$$

The three real roots of cubic equation (15) in v^2 correspond to the speeds of three quasi plane waves in a transversely isotropic micropolar piezoelectric medium. The three roots v_1, v_2 and v_3 ($v_1 > v_2 > v_3$) correspond to the speeds of Coupled Longitudinal Displacement (CLD), Coupled Transverse Displacement (CTD) and Coupled Transverse Microrotational (CTM) waves, respectively. In absence of micropolar piezoelectric fields, the equations of motion (10) to (13) reduce for transversely isotropic elastic medium M' as

$$A_{11}' \frac{\partial^2 u_1'}{\partial x^2} + (A_{13}' + A_{56}') \frac{\partial^2 u_3'}{\partial x \partial z} + A_{55}' \frac{\partial^2 u_1'}{\partial z^2} = \rho' \frac{\partial^2 u_1'}{\partial t^2}, \tag{16}$$

$$A_{66}' \frac{\partial^2 u_3'}{\partial x^2} + (A_{13}' + A_{56}') \frac{\partial^2 u_1'}{\partial x \partial z} + A_{33}' \frac{\partial^2 u_3'}{\partial z^2} = \rho' \frac{\partial^2 u_3'}{\partial t^2}. \tag{17}$$

Here the elastic parameters and displacement components with primes correspond for the transversely isotropic elastic medium. Similarly, the plane wave solution of the equations (16) to (17) shows that there exists two quasi plane waves, namely, quasi longitudinal (qP) and quasi shear vertical (qSV) waves with speeds v_1' and v_2', respectively. The speeds v_1' and v_2' ($v_1' > v_2'$) of qP and qSV waves are given by

$$v_{1,2}'^2 = \frac{\left(S_1' \pm \sqrt{S_1'^2 - 4S_2'} \right)}{2\rho'}, \tag{18}$$

where

$$S_1' = D_1' + D_2', \ S_2' = D_1' D_2' - L_1'^2,$$

$$D_1' = A_{11}' \sin^2 \theta + A_{55}' \cos^2 \theta, \ D_2' = A_{66}' \sin^2 \theta + A_{33}' \cos^2 \theta, \ L_1' = (A_{13}' + A_{56}') \sin \theta \cos \theta.$$

4   Reflection and Transmission

We consider a quasi-longitudinal (qP) wave propagating with speed v_1' through the transversely isotropic elastic solid half-space (M') is incident at the interface $z = 0$ making an angle θ_0 with z-axis. For this incident wave, we get qP and qSV waves as reflected waves in medium M' and CLD, CTD and CTM waves as transmitted waves in transversely isotropic micropolar piezoelectric medium M as shown in Fig. 1. The appropriate displacement components u_1', u_3' for incident and reflected waves in medium M' are

$$u_1' = A_0 \exp.\left\{ik_1'\left(x\sin\theta_0 + z\cos\theta_0 - v_1't\right)\right\} + \sum_{j=1}^{2} A_j' \exp.\left\{ik_j'\left(x\sin\theta_j' - z\cos\theta_j' - v_j't\right)\right\}, \tag{19}$$

$$u_3' = \xi_1^* A_0 \exp.\left\{ik_1'\left(x\sin\theta_0 + z\cos\theta_0 - v_1't\right)\right\} + \sum_{j=1}^{2} \xi_j' A_j' \exp.\left\{ik_j'\left(x\sin\theta_j' - z\cos\theta_j' - v_j't\right)\right\}. \tag{20}$$

The appropriate displacement components u_1, u_3, microrotation component ϕ_2 and electric potential ψ for transmitted waves in medium M are

$$u_1 = \sum_{j=1}^{3} A_j \exp.\left\{ik_j\left(x\sin\theta_j + z\cos\theta_j - v_j t\right)\right\}, \tag{21}$$

$$u_3 = \sum_{j=1}^{3} \xi_j A_j \exp.\left\{ik_j\left(x\sin\theta_j + z\cos\theta_j - v_j t\right)\right\}, \tag{22}$$

$$\phi_2 = \sum_{j=1}^{3} \eta_j A_j \exp.\left\{ik_j\left(x\sin\theta_j + z\cos\theta_j - v_j t\right)\right\}, \tag{23}$$

$$\psi = \sum_{j=1}^{3} \zeta_j A_j \exp.\left\{ik_j\left(x\sin\theta_j + z\cos\theta_j - v_j t\right)\right\}. \tag{24}$$

where the expressions for ξ_1^*, $\xi_j'\left(j=1,2\right)$, ξ_j, η_j and $\zeta_j\left(j=1,2,3\right)$ are given in appendix.
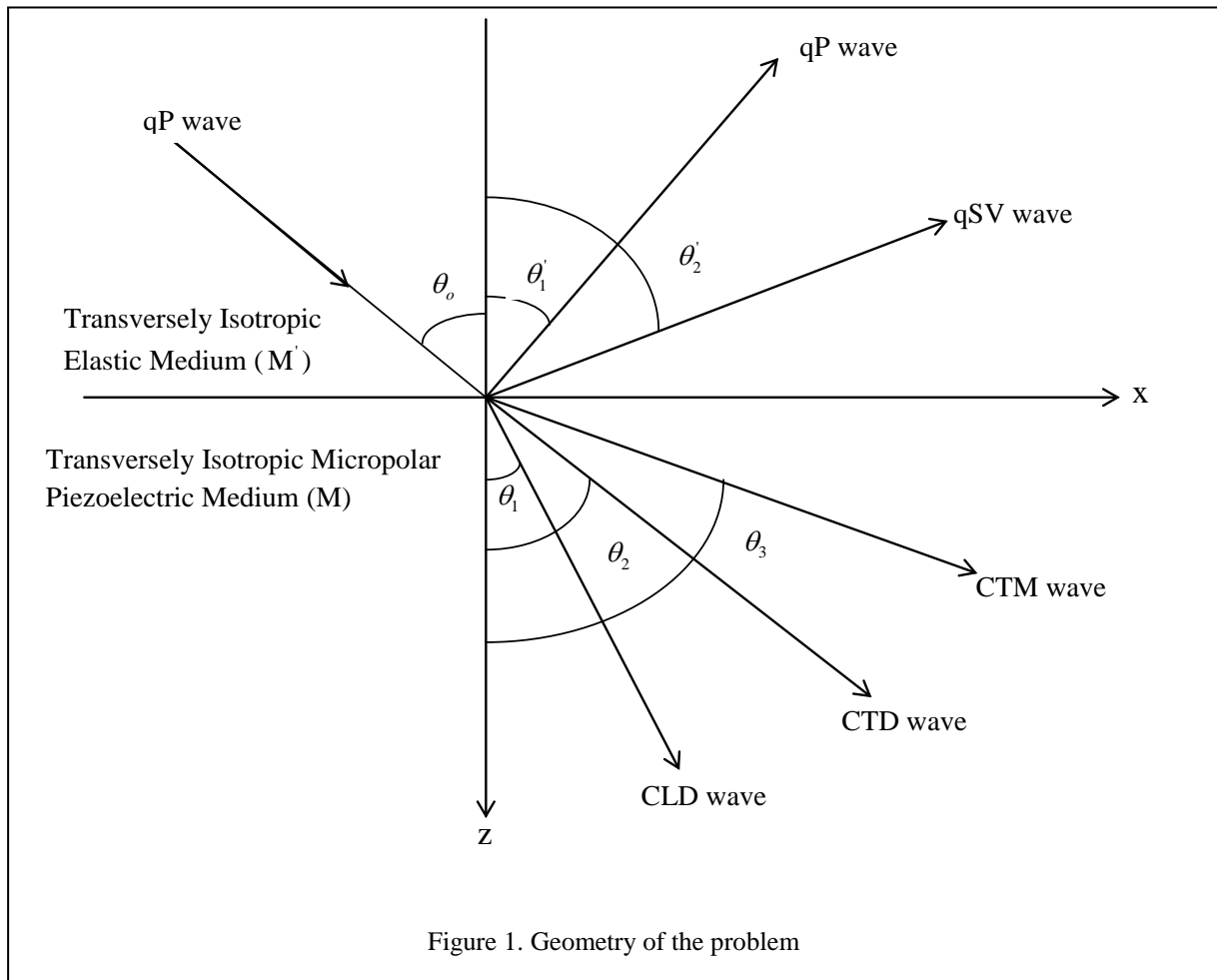
Figure 1. Geometry of the problem

5 Boundary Conditions

The appropriate boundary conditions at an interface $z = 0$ are the continuity of normal and tangential force stress components, continuity of normal component of displacement vector, vanishing of electric displacement component and vanishing of tangential couple stress component i.e.,

$$\sigma_{33} = \sigma'_{33}, \ \sigma_{31} = \sigma'_{31}, u_3 = u'_3, D_3 = 0, \ m_{32} = 0, \tag{25}$$

where

$$\sigma'_{33} = A'_{13}u'_{1,1} + A'_{33}u'_{3,3}, \ \ \sigma_{33} = A_{13}u_{1,1} + A_{33}u_{3,3} - \lambda_{35}\psi_{,1} - \lambda_{33}\psi_{,3},$$

$$\sigma'_{31} = A'_{56}u'_{3,1} + A'_{55}u'_{1,3}, \ \ \sigma_{31} = A_{56}u_{3,1} + A_{55}u_{1,3} + \left(A_{56} - A_{55}\right)\phi_2 - \lambda_{31}\psi_{,1} - \lambda_{35}\psi_{,3},$$

$$D_3 = \lambda_{15}u_{1,1} + \lambda_{33}u_{3,3} + \beta_{36}\phi_{2,3} + \gamma_{33}\psi_{,3}, \ \ m_{32} = B_{66}\phi_{2,3} - \beta_{36}\psi_{,3}.$$

The displacement components, microrotation component and electric potential functions given by equations (19) to (24) satisfy boundary conditions (25) if following relations (Snell's law) hold

$$k'_1 \sin \theta_0 = k'_1 \sin \theta'_1 = k'_2 \sin \theta'_2 = k_1 \sin \theta_1 = k_2 \sin \theta_2 = k_3 \sin \theta_3, \tag{26}$$

$$k'_1 v'_1 = k'_2 v'_2 = k_1 v_1 = k_2 v_2 = k_3 v_3, \tag{27}$$

and we obtain following non-homogeneous system of five equations in amplitude ratios of reflected and transmitted waves

$$\sum_{j=1}^{5} a_{ij}Z_j = b_i, \quad \left(i = 1, 2, ..., 5\right) \tag{28}$$

where $Z_j = \begin{cases} \dfrac{A'_j}{A_0}, & (j = 1, 2) \\ \dfrac{A_{j-2}}{A_0} & (j = 3, 4, 5) \end{cases}$ are amplitude ratios of reflected qP, qSV and transmitted CLD, CTD and CTM waves, respectively and

$$a_{1j} = \begin{cases} \dfrac{A'_{33}\xi'_j\left(\dfrac{v'_1}{v'_j}\right)\sqrt{1 - \sin^2 \theta_0 \left(\dfrac{v'_j}{v'_1}\right)^2} - A'_{13}\sin \theta_0}{A'_{13}\sin \theta_0 + A'_{33}\xi_1^*\cos \theta_0}, & (j = 1, 2) \\[4ex] \dfrac{\left(A_{13} - \lambda_{35}\zeta_{j-2}\right)\sin \theta_0 + \left(A_{33}\xi_{j-2} - \lambda_{33}\zeta_{j-2}\right)\left(\dfrac{v'_1}{v_{j-2}}\right)\sqrt{1 - \sin^2 \theta_0 \left(\dfrac{v_{j-2}}{v'_1}\right)^2}}{A'_{13}\sin \theta_0 + A'_{33}\xi_1^*\cos \theta_0}, & (j = 3, 4, 5) \end{cases}$$

$$a_{2j} = \begin{cases} \dfrac{A'_{55}\left(\dfrac{v'_1}{v'_j}\right)\sqrt{1-\sin^2\theta_0\left(\dfrac{v'_j}{v'_1}\right)^2} - A'_{56}\xi'_j\sin\theta_0}{A'_{56}\xi_1^*\sin\theta_0 + A'_{55}\cos\theta_0}, & (j=1,2) \\[4mm] \dfrac{\left(A_{56}\xi_{j-2} - \lambda_{31}\zeta_{j-2}\right)\sin\theta_0 + \left(A_{55} - \lambda_{35}\zeta_{j-2}\right)\left(\dfrac{v'_1}{v_{j-2}}\right)\sqrt{1-\sin^2\theta_0\left(\dfrac{v_{j-2}}{v'_1}\right)^2}}{} \\[2mm] \quad\dfrac{-i\left(A_{56} - A_{55}\right)\left(\dfrac{v'_1}{v_{j-2}}\right)\left(\dfrac{\eta_{j-2}}{k_{j-2}}\right)}{A'_{56}\xi_1^*\sin\theta_0 + A'_{55}\cos\theta_0}, & (j=3,4,5) \end{cases}$$

$$a_{3j} = \begin{cases} \dfrac{-\xi'_j}{\xi_1^*}, & (j=1,2) \\[3mm] \dfrac{\xi_{j-2}}{\xi_1^*}, & (j=3,4,5) \end{cases}$$

$$a_{4j} = \begin{cases} 0, & (j=1,2) \\[3mm] \lambda_{15}\sin\theta_0 + \left(\lambda_{33}\xi_{j-2} + \beta_{36}\eta_{j-2} + \gamma_{33}\zeta_{j-2}\right)\left(\dfrac{v'_1}{v_{j-2}}\right)\sqrt{1-\sin^2\theta_0\left(\dfrac{v_{j-2}}{v'_1}\right)^2}, & (j=3,4,5) \end{cases}$$

$$a_{5j} = \begin{cases} 0, & (j=1,2) \\[3mm] \left(B_{66}\eta_{j-2} - \beta_{36}\zeta_{j-2}\right)\sqrt{1-\sin^2\theta_0\left(\dfrac{v_{j-2}}{v'_1}\right)^2}, & (j=3,4,5) \end{cases}$$

$$b_i = \begin{cases} 1, & (i=1,2,3) \\ 0, & (i=4,5) \end{cases}$$

6   Expressions for Energy Ratios

We shall now consider the partitioning of energy between different reflected and transmitted waves at a surface element of unit area. Following Achenbach (1973), the instantaneous rate of work of surface traction is the scalar product of the surface traction and the particle velocity. This scalar product is called the power per unit area, denoted by P^*, and represents the rate at which the energy is communicated per unit area of the surface, i.e., the energy flux across the surface element. The time average of P^* over a period, denoted by $\left\langle P^* \right\rangle$, represents the average energy transmission per unit surface area per unit time. For the both elastic and micropolar piezoelectric media, the rate of energy transmission at the free surface $z = 0$ is given by

$$P^* = \begin{cases} \sigma'_{33}\dot{u}'_3 + \sigma'_{31}\dot{u}'_1, & \text{for medium } M' \\ \sigma_{33}\dot{u}_3 + \sigma_{31}\dot{u}_1 + m_{32}\dot{\phi}_2, & \text{for medium } M \end{cases} \tag{29}$$

The time rate of average energy transmission for the respective wave to that of the incident wave, denoted by E_j (j=1, 2... 5) for reflected qP, reflected qSV, transmitted CLD, transmitted CTD and transmitted CTM waves respectively, are given as

$$E_j = \frac{\left\langle P_j^* \right\rangle}{\left\langle P_0^* \right\rangle}, \qquad (j = 1, 2, ..., 5) \tag{30}$$

where $\left\langle P_0^* \right\rangle$ denotes the average energy transmission per unit surface area per unit time for incident qP wave in elastic medium.

The expressions for energy ratios at an interface z = 0 are given as

$$E_j = \begin{cases} \left(\dfrac{p_j' + q_j'}{w_0} \right) Z_j^2, & (j = 1, 2) \\[3mm] \left(\dfrac{p_j + q_j - r_j}{w_0} \right) Z_j^2, & (j = 3, 4, 5) \end{cases} \tag{31}$$

where

$$p_j' = (A_{13}' + A_{56}')\xi_j' \sin\theta_0, \quad q_j' = -(A_{55}' + A_{33}'\xi_j'^2)\left(\frac{v_1'}{v_j'} \right)\sqrt{1 - \sin^2\theta_0 \left(\frac{v_j'}{v_1'} \right)^2},$$

$$w_0 = (A_{13}' + A_{56}')\xi_1^* \sin\theta_0 + (A_{55}' + A_{33}'\xi_1^{*2})\cos\theta_0,$$

$$p_j = (A_{13}\xi_{j-2} + A_{56}\xi_{j-2} - \lambda_{35}\xi_{j-2}\zeta_{j-2} - \lambda_{31}\zeta_{j-2})\sin\theta_0,$$

$$q_j = (A_{55} + A_{33}\xi_{j-2}^2 - \lambda_{33}\xi_{j-2}\zeta_{j-2} - \lambda_{35}\zeta_{j-2} + B_{66}\eta_{j-2}^2 - \beta_{36}\eta_{j-2}\zeta_{j-2})\left(\frac{v_1'}{v_{j-2}} \right)\sqrt{1 - \sin^2\theta_0 \left(\frac{v_{j-2}}{v_1'} \right)^2},$$

$$r_j = i(A_{56} - A_{55})\left(\frac{v_1'}{v_{j-2}} \right)\left(\frac{\eta_{j-2}}{k_{j-2}} \right).$$

The above theoretical analysis reduces for case of TIE/TIE interface, when

$$\lambda_{33} = 0, \lambda_{35} = 0, \lambda_{31} = 0, \lambda_{15} = 0, \beta_{36} = 0, \beta_{14} = 0, \gamma_{33} = 0, \gamma_{11} = 0, K_1 = K_2 = K = 0,$$
$$A_{11} = C_{11}, A_{33} = C_{33}, \chi = 0, A_{55} = A_{66} = A_{56} = C_{44}, A_{13} = C_{13}, B_{66} = B_{77} = 0.$$

where TIE refers to transversely isotropic elastic case.

7   Numerical Results and Discussion

To the best of author's knowledge, the micromechanics based data for transversely isotropic micropolar piezoelectric materials is not available in literature. Recent studies on wave propagation in transversely isotropic micropolar media have considered theoretical values of elastic moduli, for example, Gupta and Kumar (2009); Kumar and Gupta (2010 a, b, 2012) and Abbas and Kumar (2014). In present study, the relevant values of physical constants (satisfying the inequalities among the constants) of a transversely isotropic composite material modelled as a micropolar piezoelectric medium are taken to compute the amplitude ratios and the square roots of energy ratios of reflected and transmitted waves. In present numerical example, we consider the physical data for transversely isotropic micropolar piezoelectric (TIMP) medium (M) as

$A_{11} = 17.8 \times 10^{10} \, \text{Nm}^{-2}$, $A_{33} = 18.43 \times 10^{10} \, \text{Nm}^{-2}$, $A_{13} = 7.59 \times 10^{10} \, \text{Nm}^{-2}$, $A_{56} = 1.89 \times 10^{10} \, \text{Nm}^{-2}$,

$A_{55} = 4.357 \times 10^{10} \, \text{Nm}^{-2}$, $A_{66} = 4.42 \times 10^{10} \, \text{Nm}^{-2}$, $B_{77} = 0.278 \times 10^9 \, \text{N}$, $B_{66} = 0.268 \times 10^9 \, \text{N}$,

$\lambda_{15} = 37 \, \text{Cm}^{-2}$, $\lambda_{31} = 12 \, \text{Cm}^{-2}$, $\lambda_{33} = 1.33 \, \text{Cm}^{-2}$, $\lambda_{35} = 0.23 \, \text{Cm}^{-2}$, $\beta_{14} = 0.0001 \, \text{Cm}^{-1}$, $\beta_{36} = 0.0002 \, \text{Cm}^{-1}$,

$\gamma_{11} = 0.000852 \, \text{C}^2\text{N}^{-1}\text{m}^{-2}$, $\gamma_{33} = 0.000287 \, \text{C}^2\text{N}^{-1}\text{m}^{-2}$, $\rho = 1.74 \times 10^3 \, \text{Kg}\,\text{m}^{-3}$, $j = 0.196 \, \text{m}^2$.

Following physical constants for transversely isotropic elastic (TIE) medium ($M^{'}$) are also considered

$$A_{11}^{'}=16.8\times10^{10}\,\mathrm{Nm^{-2}},\ A_{33}^{'}=17.43\times10^{10}\,\mathrm{Nm^{-2}},\ A_{13}^{'}=7.2\times10^{10}\,\mathrm{Nm^{-2}},$$
$$A_{56}^{'}=1.29\times10^{10}\,\mathrm{Nm^{-2}},\ A_{55}^{'}=4.157\times10^{10}\,\mathrm{Nm^{-2}},\ A_{66}^{'}=4.1\times10^{10}\,\mathrm{Nm^{-2}},\ \rho^{'}=1.2\times10^{3}\,\mathrm{Kg\,m^{-3}}.$$

For above theoretical values of physical constants, the equations (28) and (31) are solved numerically with the help of MATLAB. The absolute value of amplitude ratios and the square root of energy ratios of various reflected and transmitted waves are computed. To check the correctness of code implementation, the variations of computed amplitude ratios and energy ratios are verified with earlier established results in Ewing et al. (1957) and Achenbach (1973).

The amplitude ratios of reflected qP, qSV and transmitted CLD, CTD and CTM waves are plotted for range $0^{0}<\theta_{0}<90^{0}$ of the angle of incidence of qP wave in Figs. 2-6. The solid and dotted curves in Figs. 2-6 correspond to variations of reflection and transmission coefficients for cases of TIE/TIMP interface and TIE/TIE interface, respectively. For case of TIE/TIMP interface, the amplitude ratio of reflected qP wave is obtained as 0.1065 at angle of incidence $\theta_{0}=0.1^{o}$ (near normal incidence). It increases slowly to value 0.1439 at $\theta_{0}=26.2247^{o}$ and then decreases with the increase in angle of incidence and attains its minimum value 2.8683×10^{-5} at $\theta_{0}=58.9782^{o}$. Thereafter, it increases sharply to value 0.9999 at $\theta_{0}=89.9998^{o}$ (near grazing incidence). For case of TIE/TIE interface, the amplitude ratio of reflected qP wave is obtained as 0.1064 at $\theta_{0}=0.1^{o}$. It increases slowly to value 0.1532 at $\theta_{0}=29.7000^{o}$ and then decreases with the increase in angle of incidence and attains its minimum value 5.9571×10^{-8} at $\theta_{0}=49.8520^{o}$. Thereafter, it increases sharply to value 0.9999 at $\theta_{0}=89.9998^{o}$. For case of TIE/TIMP interface, the amplitude ratio of reflected qSV wave is obtained 0.3886 at $\theta_{0}=0.1^{o}$. It increases to maximum value 0.3963 at $\theta_{0}=0.6479^{o}$ and then decreases sharply with increase in angle of incidence and attains value 4.4322×10^{-5} at $\theta_{0}=59.7381^{o}$. Thereafter, it increases slowly to value 0.0099 at $\theta_{0}=70.6703^{o}$ and then decreases to value 1.0151×10^{-7} at $\theta_{0}=89.9998^{o}$. For case of TIE/TIE interface, the amplitude ratio of reflected qSV wave is obtained 0.3536 at $\theta_{0}=0.1^{o}$. It increases to its maximum value 0.4096 at $\theta_{0}=31.3546^{o}$. Thereafter, it decreases and attains value 5.5576×10^{-7} at $\theta_{0}=89.9998^{o}$. For case of TIE/TIMP interface, the amplitude ratio of transmitted CLD wave is obtained 0.7949 at $\theta_{0}=0.1^{o}$. It increases to its maximum value 0.7949 at $\theta_{0}=0.1064^{o}$. Thereafter, it decreases with increase in angle of incidence and attains value 3.8589×10^{-6} at $\theta_{0}=89.9998^{o}$. For case of TIE/TIE interface, the maximum value of amplitude ratio of transmitted CLD wave is obtained 1.0127 at $\theta_{0}=0.1^{o}$. Thereafter, it decreases with increase in angle of incidence and attains value 3.1009×10^{-6} at $\theta_{0}=89.9998^{o}$. For case of TIE/TIMP interface, the amplitude ratio of transmitted CTD wave is obtained 0.1589 at angle of incidence $\theta_{0}=0.1^{o}$. It increases to its maximum value 0.2667 at $\theta_{0}=14.7229^{o}$ and then decreases sharply with increase in incidence angle and attains value 1.1411×10^{-5} at $\theta_{0}=54.9929^{o}$. Thereafter, it increases to value 0.0207 at $\theta_{0}=70.1918^{o}$ and then again decreases to value 2.2206×10^{-7} at $\theta_{0}=89.9998^{o}$. For case of TIE/TIE interface, the maximum value of amplitude ratio of transmitted CTD wave attains 0.2599 at $\theta_{0}=0.1^{o}$ and then decreases to value 3.0585×10^{-7} at $\theta_{0}=44.5767^{o}$. Thereafter, it increases to value 0.0751 at $\theta_{0}=62.8282^{o}$ and then again decreases to value 5.0267×10^{-7} at $\theta_{0}=89.9998^{o}$. For case of TIE/TIMP interface, the amplitude ratio of transmitted CTM wave is obtained 0.0526 at $\theta_{0}=0.1^{o}$. It increases to its maximum value 0.0537 at $\theta_{0}=0.3841^{o}$ and then decreases to value 0.0059 at $\theta_{0}=45.4320^{o}$. Thereafter, it increases to value 0.0119 at $\theta_{0}=69.0348^{o}$ and then decreases to value 1.2651×10^{-7} at $\theta_{0}=89.9998^{o}$. For case of TIE/TIE interface, there is no transmitted CTM wave. Comparing the solid curves with dotted curves, the effects of micropolarity and piezoelectricity are observed significant on amplitude ratios of various reflected and transmitted waves. Also, the amplitude ratios of all reflected and transmitted waves change with change in angle of incidence.
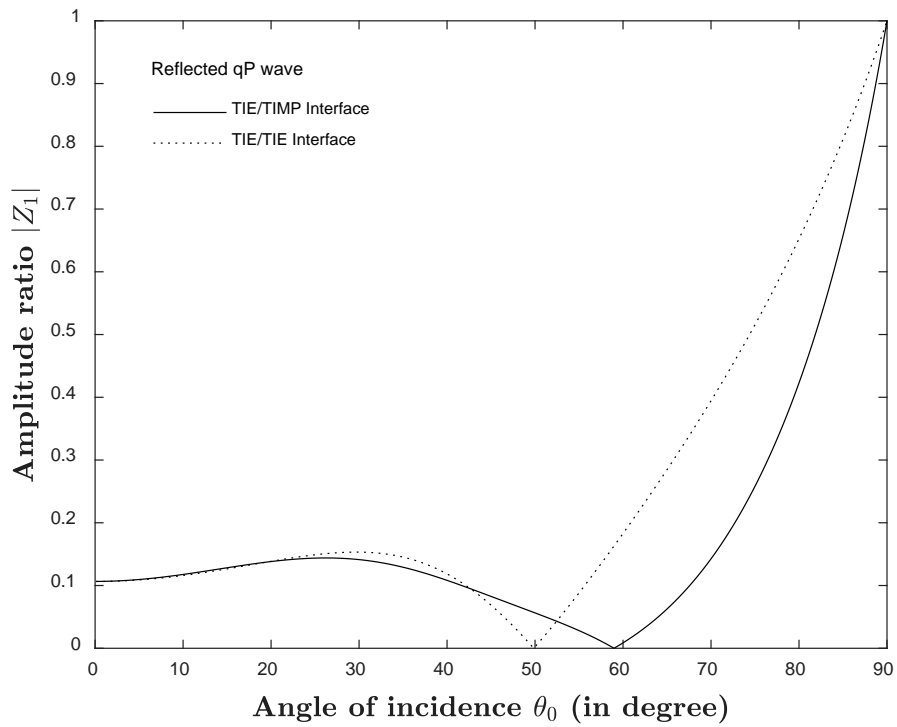
Figure 2. Variations of the amplitude ratios of reflected quasi-longitudinal (qP) wave against the angle of incidence of incident qP wave
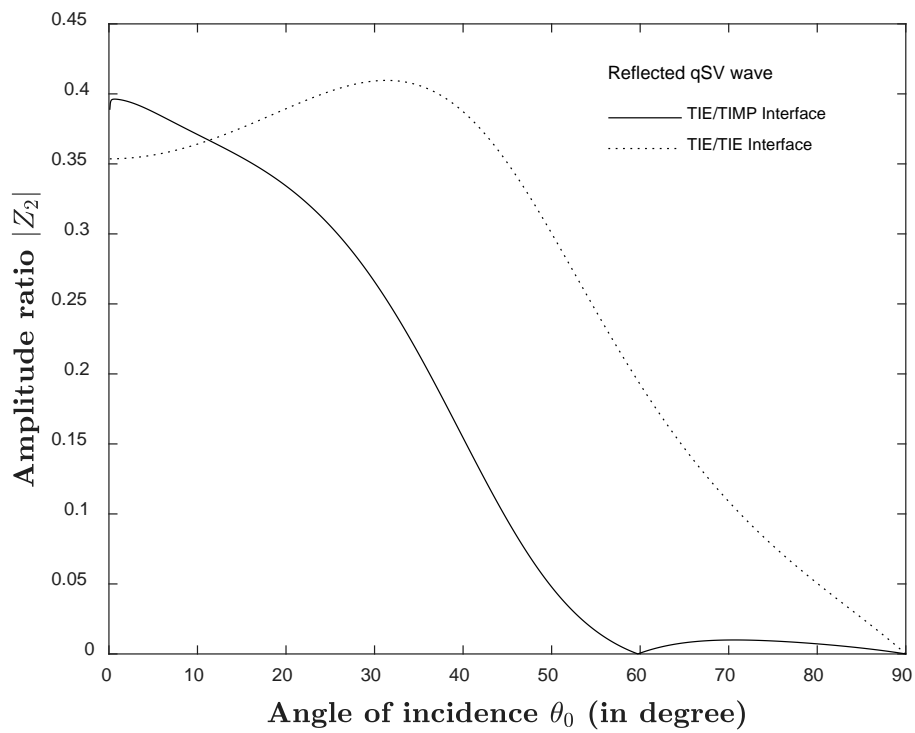
Figure 3. Variations of the amplitude ratios of reflected quasi-shear vertical (qSV) wave against the angle of incidence of incident qP wave

276
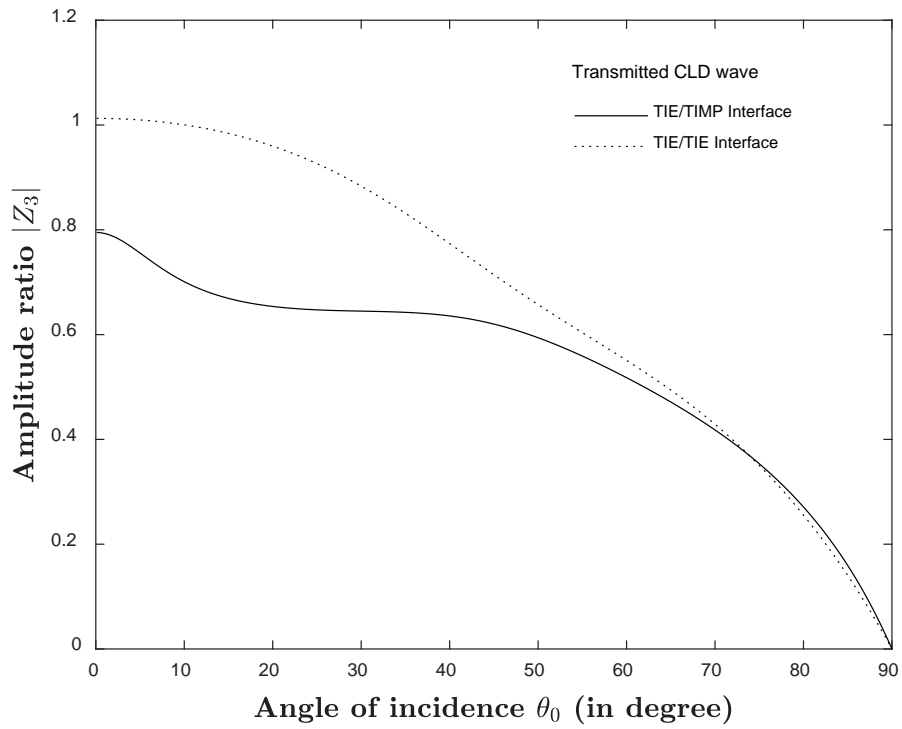
Figure 4. Variations of the amplitude ratios of transmitted coupled longitudinal displacement (CLD) wave against the angle of incidence of incident qP wave
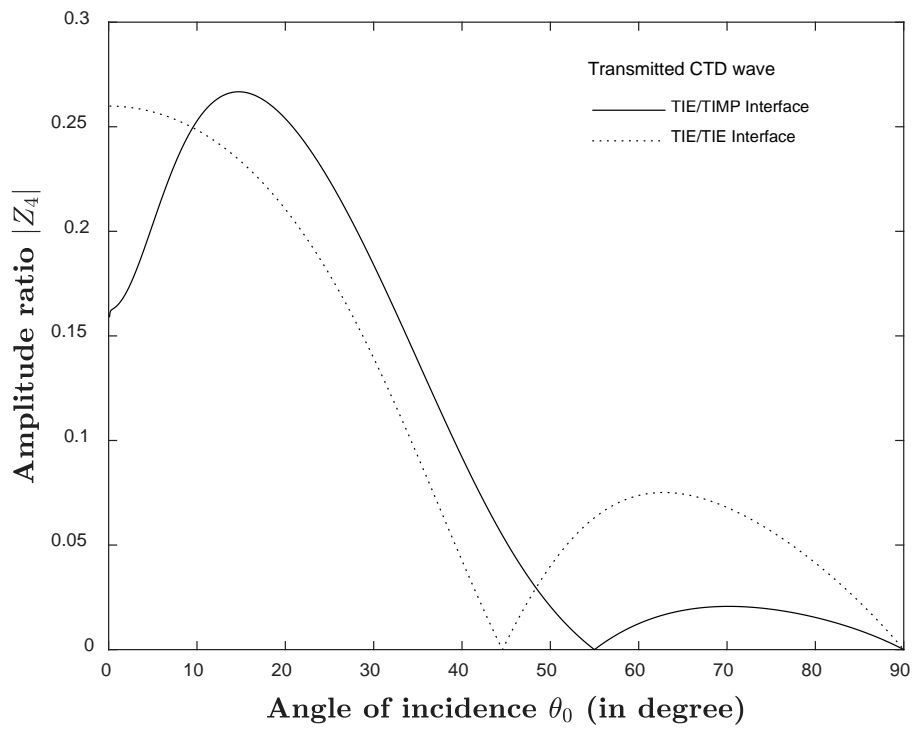
Figure 5. Variations of the amplitude ratios of transmitted coupled transverse displacement (CTD) wave against the angle of incidence of incident qP wave
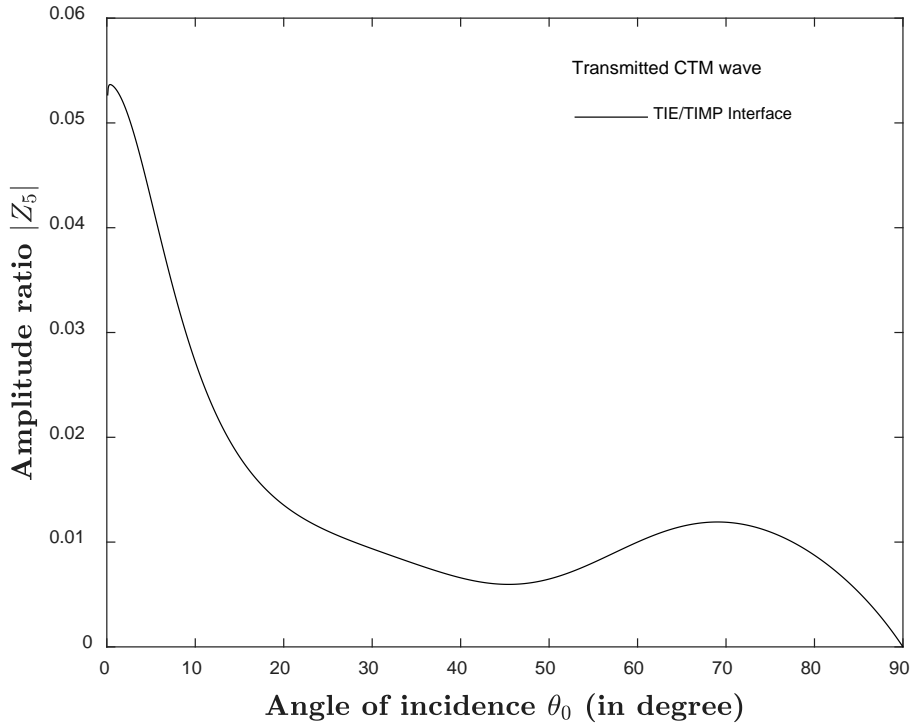
Figure 6. Variations of the amplitude ratios of transmitted coupled transverse microrotational (CTM) wave against the angle of incidence of incident qP wave

The square root of energy ratios of reflected qP, qSV and transmitted CLD, CTD and CTM waves are plotted for range $0^0 < \theta_0 < 90^0$ of the angle of incidence of qP wave in Figs. 7-11. The solid and dotted curves in Figs. 7-11 correspond to variation of the square root of energy ratios of various reflected and transmitted waves for cases of TIE/TIMP interface and TIE/TIE interface, respectively. For case of TIE/TIMP interface, the square root of energy ratio of reflected qP wave is obtained as 0.1064 at angle of incidence $\theta_0 = 0.0001^o$ (near normal incidence). It increases slowly to value 0.1439 at $\theta_0 = 26.2247^o$ and then decreases with the increase in angle of incidence and attains its minimum value 2.8683×10^{-5} at $\theta_0 = 58.9782^o$. Thereafter, it increases sharply to value 0.9999 at $\theta_0 = 89.9998^o$ (near grazing incidence). For case of TIE/TIE interface, the square root of energy ratios of reflected qP wave is obtained as 0.1064 at $\theta_0 = 0.0001^o$. It increases slowly to value 0.1532 at $\theta_0 = 29.7000^o$ and then decreases with the increase in angle of incidence and attains its minimum value 5.9571×10^{-8} at $\theta_0 = 49.8520^o$. Thereafter, it increases sharply to value 0.9999 at $\theta_0 = 89.9998^o$. For case of TIE/TIMP interface, the square root of energy ratio of reflected qSV wave is obtained 0.1066×10^{-6} at angle of incidence $\theta_0 = 0.0001^o$. It increases sharply to its maximum value 0.0786 at $\theta_0 = 30.2565^o$ and then decreases to value 4.6706×10^{-5} at $\theta_0 = 59.7381^o$. Thereafter, it increases to value 0.0243 at $\theta_0 = 79.2659^o$ and then decreases to value 1.2259×10^{-4} at $\theta_0 = 89.9998^o$. For case of TIE/TIE interface, the square root of energy ratio of reflected qSV wave is obtained 2.7587×10^{-7} at $\theta_0 = 0.0001^o$. It increases to value 0.2097 at $\theta_0 = 64.9461^o$ and then decreases to value 6.4046×10^{-4} at $\theta_0 = 89.9998^o$. For case of TIE/TIMP interface, the square root of energy ratio of transmitted CLD wave is obtained 0.9943 at $\theta_0 = 0.0001^o$. It increases to value 0.9951 at $\theta_0 = 0.3562^o$ and then decreases to value 0.9921 at $\theta_0 = 17.5078^o$. Thereafter, it increases to its maximum value 0.9979 at $\theta_0 = 34.6312^o$ and then decreases to value 0.0035 at $\theta_0 = 89.9998^o$. For case of TIE/TIE interface, the square root of energy ratio of transmitted CLD wave is obtained 0.9943 at $\theta_0 = 0.0001^o$. It decreases to value

2.9966×10^{-3} at $\theta_0 = 89.9998^o$. For case of TIE/TIMP interface, the square root of energy ratio of transmitted CTD wave is obtained 5.0764×10^{-6} at angle of incidence $\theta_0 = 0.0001^o$. It increases to its maximum value 0.0662 at $\theta_0 = 32.9946^o$ and then decreases sharply with increase in incident angle and attains value 1.6062×10^{-5} at $\theta_0 = 54.9929^o$. Thereafter, it increases to value 0.0493 at $\theta_0 = 76.3905^o$ and then again decreases to value 2.2918×10^{-4} at $\theta_0 = 89.9998^o$. For case of TIE/TIE interface, the square root of energy ratio of transmitted CTD wave is obtained 2.2512×10^{-7} at $\theta_0 = 0.0001^o$. It increases to value 0.0445 at $\theta_0 = 26.9488^o$ and then decreases to value 1.7880×10^{-7} at $\theta_0 = 44.5776^o$. Thereafter, it increases to maximum value 0.1188 at $\theta_0 = 74.8593^o$ and then again decreases to value 4.5305×10^{-4} at $\theta_0 = 89.9998^o$. For case of TIE/TIMP interface, the square root of energy ratio of transmitted CTM wave is obtained 1.4592×10^{-6} at $\theta_0 = 0.0001^o$. It increases to value 2.7747×10^{-4} at $\theta_0 = 0.2716^o$. Thereafter, it also increases to its maximum value 0.0221 at $\theta_0 = 78.0819^o$ and then decreases to value 1.0837×10^{-4} at $\theta_0 = 89.9998^o$. Comparing solid curves with dotted curves, it is observed that the square root of energy ratios of various reflected and transmitted waves are significantly affected due to the presence of micropolarity and piezoelectricity in the lower medium. Also, the square root of energy ratios of all reflected and transmitted waves change with change in angle of incidence.
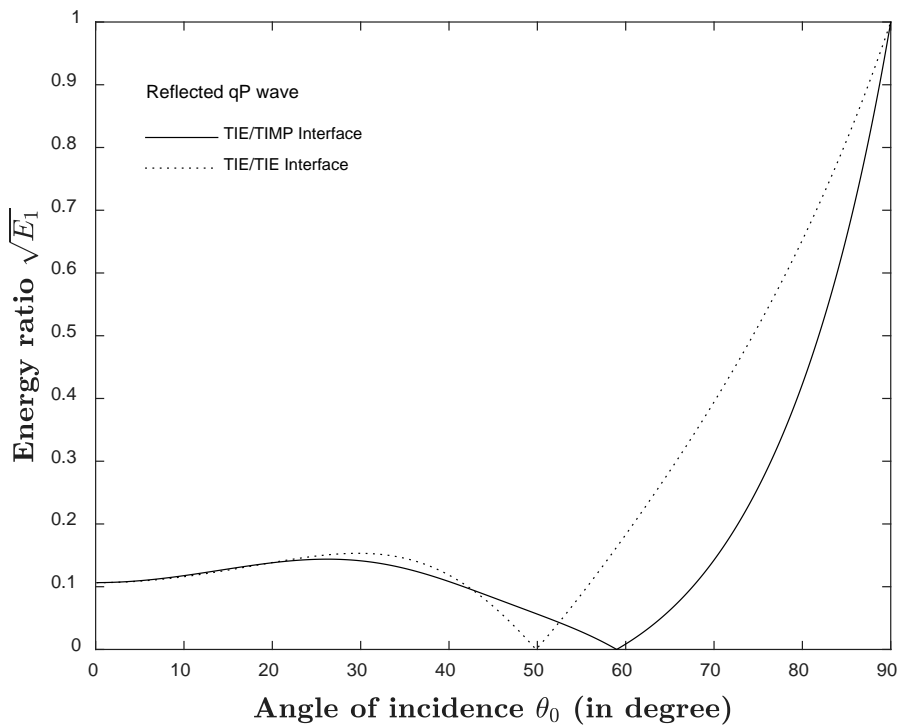
Figure 7.   Variations of the square root of energy ratios of reflected quasi-longitudinal (qP) wave against the angle of incidence of incident qP wave
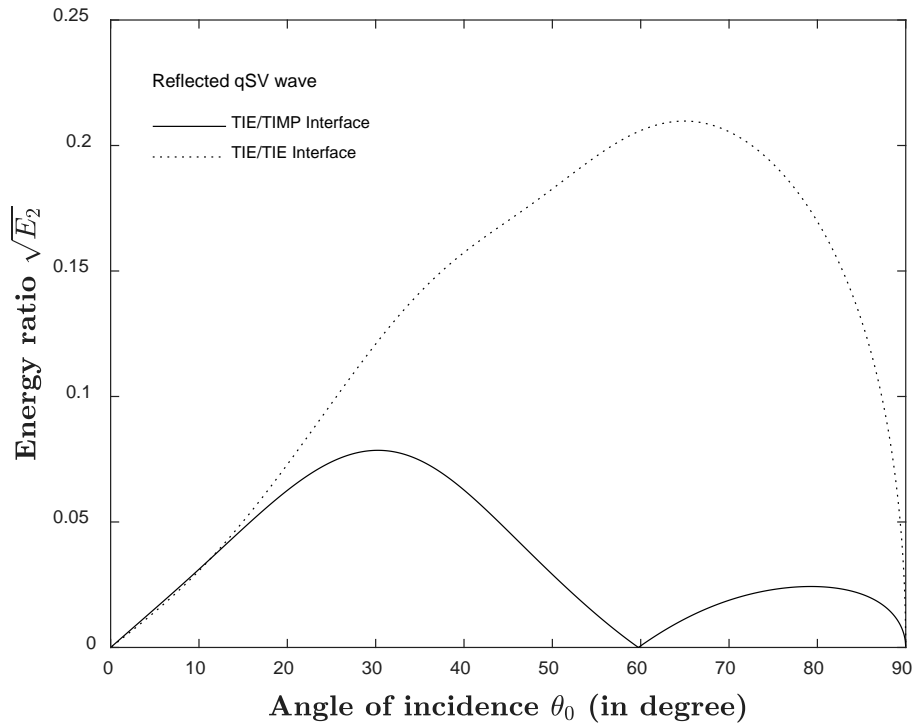
Figure 8. Variations of the square root of energy ratios of reflected quasi-shear vertical (qSV) wave against the angle of incidence of incident qP wave
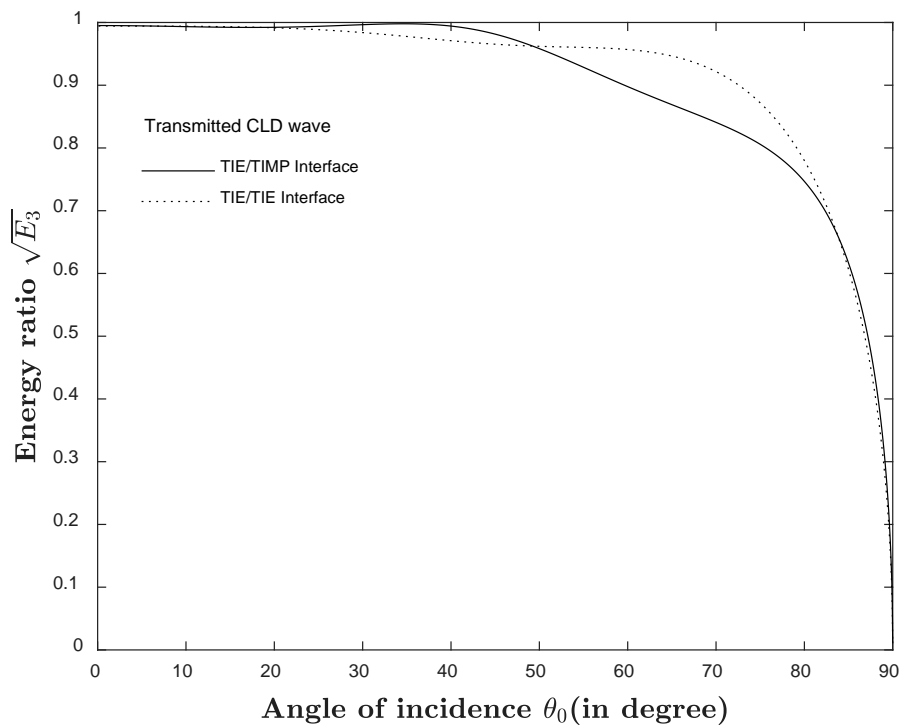
Figure 9. Variations of the square root of energy ratios of transmitted coupled longitudinal displacement (CLD) wave against the angle of incidence of incident qP wave
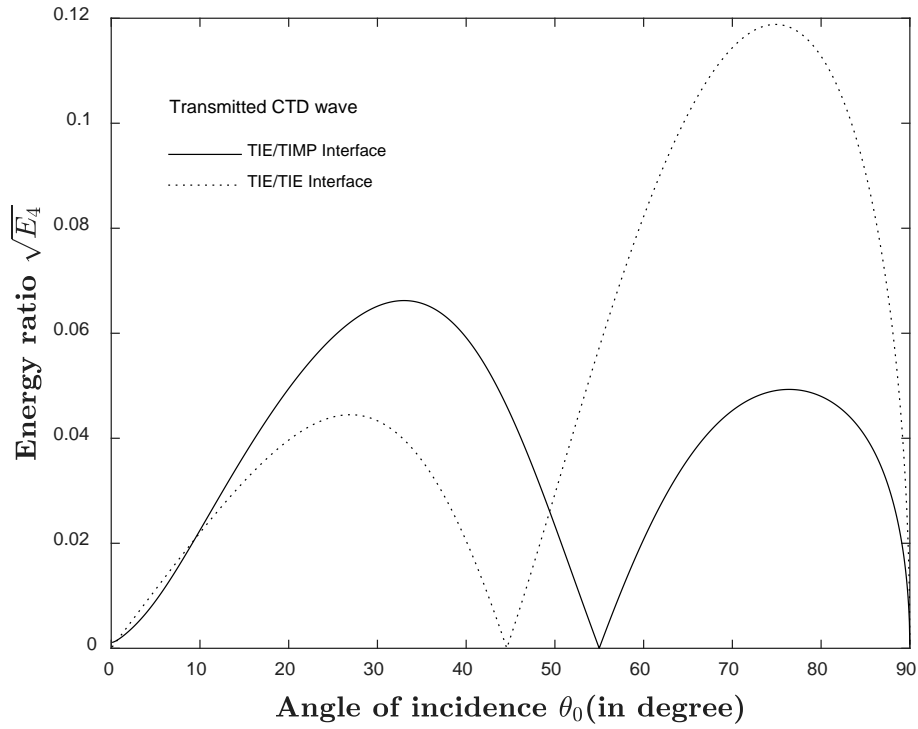
Figure 10. Variations of the square root of energy ratios of transmitted coupled transverse displacement (CTD) wave against the angle of incidence of incident qP wave
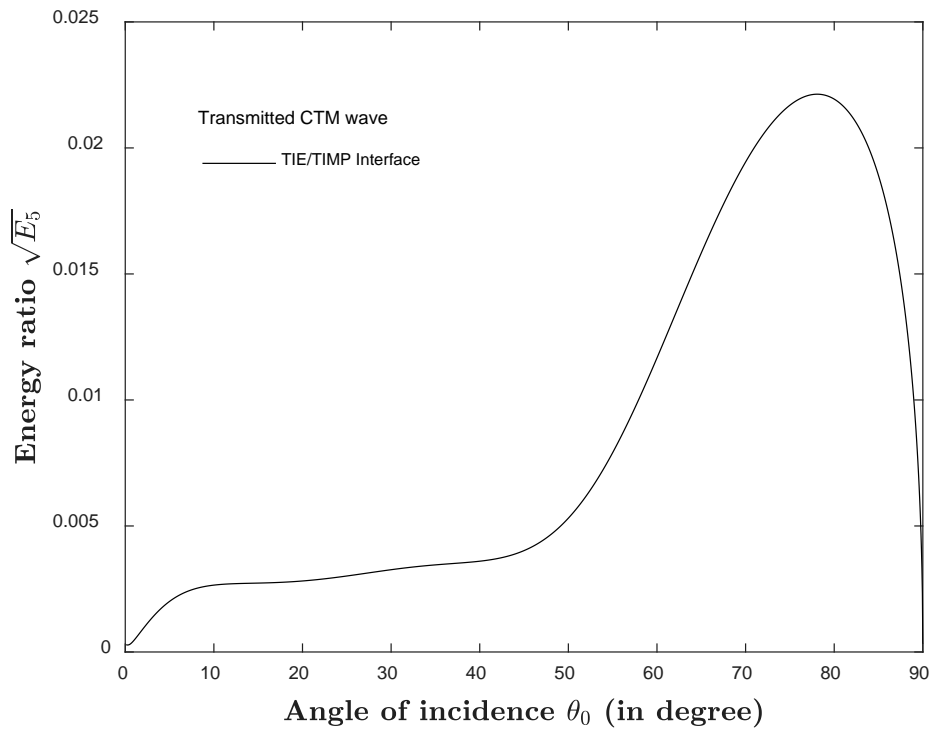
Figure 11. Variations of the square root of energy ratios of transmitted coupled transverse microrotational (CTM) wave against the angle of incidence of incident qP wave

8   Conclusion

Plane wave solutions indicate the existence of two plane waves (qP and qSV) waves in transversely isotropic elastic medium and three plane waves (CLD, CTD and CTM) waves in transversely isotropic micropolar piezoelectric medium. A problem on reflection and transmission between a transversely isotropic elastic solid half-space lying over a transversely isotropic micropolar piezoelectric solid half-space is considered for incidence of qP wave at plane interface. The relations between amplitude ratios and the expressions for the energy ratios of various reflected and transmitted waves are obtained analytically. A numerical example of the model is taken for computation of amplitude ratios and the square root of energy ratios of reflected and transmitted waves. From above numerical results and discussion, it is observed that the amplitude ratios as well as the energy ratios of all reflected and transmitted waves are affected significantly due to the presence of piezoelectric and micropolar fields. The present study is supposed to be useful in further studies on wave propagation in the more realistic models of piezoelectric and micropolar elastic solids which have been extensively used in many engineering and industrial applications such as computer technology, actuators, sensors, radio, intelligent structures and ultrasonic.

9   Appendix

The expressions for ξ_1^*, $\xi_p^{'}\left(p=1,2\right)$, ξ_p, η_p and $\zeta_p\left(p=1,2,3\right)$ using Snell's law are given as

$$\xi_1^* = -\xi_1^{'}, \ \xi_p^{'} = \frac{P_p^{'}}{Q_p^{'}}, \ \xi_p = \frac{\Delta_{1p}}{\Delta_p}, \ \frac{\eta_p}{k_p} = \frac{\Delta_{2p}}{\Delta_p}, \ \zeta_p = \frac{\Delta_{3p}}{\Delta_p},$$

where

$$P_p^{'} = A_{11}^{'}\sin^2\theta_0\left(\frac{v_p^{'}}{v_1^{'}}\right)^2 + A_{55}^{'}\left[1-\sin^2\theta_0\left(\frac{v_p^{'}}{v_1^{'}}\right)^2\right] - \rho^{'}v_p^{'\,2},$$

$$Q_p^{'} = \left(A_{13}^{'}+A_{56}^{'}\right)\sin\theta_0\left(\frac{v_p^{'}}{v_1^{'}}\right)\sqrt{1-\sin^2\theta_0\left(\frac{v_p^{'}}{v_1^{'}}\right)^2},$$

$$\Delta_p = C_pW_pK_{2p} - C_pR_pT_p - Q_pW_pK_{1p} + M_pQ_pR_p + T_pK_{1p}K_{2p}^* - M_pK_{2p}K_{2p}^*,$$

$$\Delta_{1p} = P_pW_pK_{2p} - P_pR_pT_p - C_pW_pK_{1p} + M_pC_pR_p + T_pK_{1p}K_{1p}^* - M_pK_{1p}^*K_{2p},$$

$$\Delta_{2p} = C_p^2W_p - C_pT_pK_{1p}^* - P_pQ_pW_p + P_pT_pK_{2p}^* + M_pQ_pK_{1p}^* - M_pC_pK_{2p}^*,$$

$$\Delta_{3p} = 2C_pK_{1p}K_{2p}^* - R_pC_p^2 - Q_pK_{1p}K_{1p}^* + P_pQ_pR_p - P_pK_{2p}K_{2p}^*,$$

$$P_p = \rho v_p^2 - A_{11}\sin^2\theta_0\left(\frac{v_p}{v_1^{'}}\right)^2 - A_{55}\left[1-\sin^2\theta_0\left(\frac{v_p}{v_1^{'}}\right)^2\right],$$

$$Q_p = \rho v_p^2 - A_{66}\sin^2\theta_0\left(\frac{v_p}{v_1^{'}}\right)^2 - A_{33}\left[1-\sin^2\theta_0\left(\frac{v_p}{v_1^{'}}\right)^2\right],$$

$$R_p = \frac{B_{77}}{j}\sin^2\theta_0\left(\frac{v_p}{v_1^{'}}\right)^2 + \frac{B_{66}}{j}\left[1-\sin^2\theta_0\left(\frac{v_p}{v_1^{'}}\right)^2\right] + \frac{\chi}{jk_p^2} - \rho v_p^2,$$

$$T_p = \lambda_{15}\sin^2\theta_0\left(\frac{v_p}{v_1^{'}}\right)^2 + \lambda_{33}\left[1-\sin^2\theta_0\left(\frac{v_p}{v_1^{'}}\right)^2\right],$$

$$W_p = -\left\{ \frac{\beta_{14}}{jk_p} \sin^2 \theta_0 \left(\frac{v_p}{v_1'}\right)^2 + \frac{\beta_{36}}{jk_p}\left[1 - \sin^2 \theta_0 \left(\frac{v_p}{v_1'}\right)^2\right]\right\},$$

$$C_p = \left(A_{13} + A_{56}\right)\sin\theta_0 \left(\frac{v_p}{v_1'}\right)\sqrt{1 - \sin^2 \theta_0 \left(\frac{v_p}{v_1'}\right)^2}, \quad M_p = -\left(\lambda_{15} + \lambda_{31}\right)\sin\theta_0 \left(\frac{v_p}{v_1'}\right)\sqrt{1 - \sin^2 \theta_0 \left(\frac{v_p}{v_1'}\right)^2},$$

$$K_{1p} = -iK_1 \sqrt{1 - \sin^2 \theta_0 \left(\frac{v_p}{v_1'}\right)^2}, \quad K_{2p} = iK_2 \sin\theta_0 \left(\frac{v_p}{v_1'}\right),$$

$$K_{1p}^* = -i\frac{K_1}{jk_p^2}\sqrt{1 - \sin^2 \theta_0 \left(\frac{v_p}{v_1'}\right)^2}, \quad K_{2p}^* = i\frac{K_2}{jk_p^2}\sin\theta_0 \left(\frac{v_p}{v_1'}\right).$$

10 Acknowlegment

References

Abbas, I.A.; Kumar, R.: Interaction due to a mechanical source in transversely isotropic micropolar media, *J. Vibrat. Control*, 20, (2014), 1663-1670.

Abd-alla, A.N.; Al-sheikh, F.A.: Reflection and refraction of plane quasi-longitudinal waves at an interface of two piezoelectric media under initial stress, *Arch. Appl. Mech.*, 79, (2009 a), 843-857.

Abd-alla, A.N.; Al-sheikh, F.A.: The effect of the initial stresses on the reflection and transmission of plane quasi-vertical transverse waves in piezoelectric materials, *Proceeding of World Academy of Science, Engineering and Technology*, 38, (2009 b), 660-668.

Achenbach, J.D.: *Wave propagation in elastic solids*, Vol. 16, North-Holland Publishing Company, Amsterdam, Elsevier, (1973).

Aouadi, M.: Aspects of uniqueness in micropolar piezoelectric bodies, *Mathematics and Mechanics of Solids*, 13, (2008), 499-512.

Ariman, T.: Wave propagation in a micropolar elastic half-space, *Acta. Mech.*, 13, (1972), 11-20.

Auld, B.A.: *Acoustic Fields and Waves in Solids*, Wiley Interscience, New York, 2, (1973).

Chai, J.F.; Wu, T.T.: Propagation of surface waves in a prestressed piezoelectric material, *J. Acoust. Soc. Am.*, 100, (1966), 2112-2122.

Ciumasu, S.G.; Vieru, D.: Variational formulations for the vibration of a micropolar piezoelectric body, *J. Acoust. Soc. Am.*, 105, (1999), 1240-1245.

Cracium, I.A.: Uniqueness theorem in the linear theory of piezoelectric micropolar thermoelasticity ion, *Int. J. Engng.* Sc., 33, (1995), 1027-1036.

Eremeyev, V.A.; Lebedev, L.P.; Altenbach, H.: *Foundations of micropolar mechanics*, Springer Science & Business Media, (2013).

Ergin, K.: Energy ratio of the seismic waves reflected and refracted at a rock-water boundary, condensed from a Ph.D. dissertation at the California Institute of Technology, *Bull. Seismol. Soc. Am.*, 42, (1950), 349-372.

Eringen, A.C. : Theory of micropolar elasticity, in *Fracture*, Vol 2, Academic Press, (1968), 621-729.

Eringen, A.C.: Linear theory of micropolar elasticity, *J. Math. Mech.*, 15, (1966), 909-923.

Eringen, A.C.: Microcontinuum Field Theories I: *Foundations and Soilds*, Springer, New York, (1999).

Eringen, A.C.: Microcontinuum field theories: I. *Foundations and solids*, Springer Science & Business Media, (2012).

Ewing, W.M.; Jardetzky, W.S.; Press, F.: *Elastic waves in layered Media*, McGraw-Hill Company, Inc., New York, Toronto, London, (1957).

Gales, C.: Some results in micromorphic piezoelectricity, *European Journal of Mechanics* A/Solids, 31, (2012), 37-46.

Guo, X.; Wei, P.: Effects of initial stress on the reflection and transmission waves at the interface between two piezoelectric half spaces, *Int. J. Solids. Struct.*, 51, (2014), 3735-3751.

Gupta, R.R.; Kumar, R.: Analysis of wave motion in micropolar transversely isotropic medium, *J. Solid. Mech.*, 1, (2009), 260-270.

Gutenberg, B.: Energy ratio of reflected and refracted seismic waves, *Bull. Seismol. Soc. Am.*, 38, (1944), 85-102.

Hruska, K.: The rate of propagation of Ultrasonic waves in ADP in Voigt's theory, *Czechoslovak Journal of Physics B*, 16, (1966), 446-454.

Huang, G.Y.; Yu, S.W.: Size effect of a crack in a micropolar piezoelectric medium, *Key Engineering Materials*, 417-418, (2010), 525-528.

Jeffreys, H.: The reflection and refraction of elastic waves, *Mon. Not. Roy. Astron. Soc., Geophys. Suppl.*, 1, (1926), 321-334.

Knott, C.G.: Reflection and refraction of elastic waves with seismological applications, *Philos. Mag. Ser.*, 48, (1899), 64-97.

Kuang, Z.B.; Yuan, X.G.: Reflection and transmission of waves in pyroelectric and piezoelectric materials, *J. Sound Vibr.*, 330, (2011), 1111-1120.

Kumar, R.; Gupta, R.R.: Plane waves reflection in micropolar transversely isotropic generalized thermoelastic half-space, *Math. Sci.*, 6, (2012), 1-7.

Kumar, R.; Gupta, R.R.: Reflection of waves in transversely isotropic micropolar thermoelastic half-space, *Canadian Appl. Math. Quart.*, 18, (2010 a), 393-413.

Kumar, R.; Gupta, R.R: Propagation of waves in transversely isotropic micropolar generalized thermoelastic half-space, *Int. Commun. Heat Mass Transf.*, 37, (2010 b), 1452-1458.

Kyame, J.J.: Wave Propagation in piezoelectric crystals, *J. Acoust. Soc.* Am., 21, (1949), 159-167.

Nowacki, W.: *Theory of asymmetric elasticity*, Pergamon Press, (1986).

Pailloux, P.M.H.: Piezoelectric Itecalcul Des Vitesses De Propagation, Le Journal De Physique Etle Radium, 19, (1958), 523-526.

Pang, Y.; Wang, Y.S.; Liu, J.X.; Fang, D.N.: Reflection and refraction of plane waves at the interface between piezoelectric and piezomagnetic media*, Int. J. Engng. Sc.*, 46, (2008), 1098-1110.

Parfitt, V.R.; Eringen, A.C. : Reflection of plane waves from a flat boundary of a micropolar elastic half-space, *J. Acoust. Soc. Am.*, 45, (1969), 1258-1272.

Singh, B.: Wave propagation in a prestressed piezoelectric half-space, *Acta. Mech.*, 211, (2010), 337-344.

Singh, B.; Goyal, M.: Wave propagation in a transversely isotropic microstretch elastic solid, *Mechanics of Advanced Materials and Modern Process*, 3, (2017), 1-10.

Singh, B.; Sindhu, R.: On propagation of Rayleigh type surface wave in a micropolar piezoelectric medium, *Open Journal of Acoustics*, 6, (2016), 35-44.

Smith, A.C.: Waves in micropolar elastic solids, *Int. J. Engng. Sc.*, 5, (1967), 741-746.

Tomar, S.K.; Gogna, M.L.: Reflection and refraction of longitudinal wave at an interface between two micropolar elastic solids in welded contact, *J. Acoust. Soc. Am.* , 97, (1995), 822-830.

Wang, Q.: Wave propagation in a piezoelectric coupled solid medium, *J. Appl. Mech.*, 69, (2002), 819-824.

Yang, J.S.: A review of a few topics in piezoelectricity, *Applied Mechanics Reviews*, 59, (2006), 335-345.

Yuan, X.; Zhu, Z.H.: Reflection and refraction of plane waves at interface between two piezoelectric media, *Acta. Mech.*, 223, (2012), 2509-2521.

Zhilin, P.A.; Kolpakov, Y.E.: A micro-polar theory for piezoelectric materials // Lecture at XXXIII Summer School – Conference "Advanced Problems in Mechanics", St, Petersburg, Russia, (2005)

_____

Addresses:
Asha Sangwan, Department of Mathematics, Maharshi Dayanand University, Rohtak-124001, Haryana, India.
*Baljeet Singh, Department of Mathematics, Post Graduate Government College, Sector 11, Chandigarh - 160011, India. (Corresponding Author)
Jagdish Singh, Department of Mathematics, Maharshi Dayanand University, Rohtak-124001, Haryana, India.
Email: aashisangwan53@gmail.com, bsinghgc11@gmail.com, jsnandal2k15@gmail.com